

## Electronic Supplementary Material

### Self-Assembly of 2D-Metal-Organic Frameworks/Graphene Oxide Membranes as Highly Efficient Adsorbent for the Removal of Cs<sup>+</sup> from Aqueous Solutions

Junye Cheng,<sup>a,b,1</sup> Jie Liang,<sup>a,1</sup> Liubing Dong,<sup>c</sup> Jixing Chai,<sup>d</sup> Ning Zhao,<sup>b</sup> Sana Ullah,<sup>e</sup> Hao Wang,<sup>b,\*</sup>

Deqing Zhang,<sup>d</sup> Sumair Imtiaz,<sup>e</sup> Guangcun Shan,<sup>a,\*</sup> Guangping Zheng<sup>e,\*</sup>

<sup>a</sup> School of Instrumentation Science and Opto-electronics Engineering, Beihang University, No.37

XueYuan Road, Beijing 100095, China

<sup>b</sup> Guangdong Provincial Key Laboratory of Micro/Nano Optomechatronics Engineering, College of

Mechatronics and Control Engineering, Shenzhen University, Shenzhen 518060, China

<sup>c</sup> Graduate School at Shenzhen, Tsinghua University, Shenzhen 518055, China

<sup>d</sup> School of Materials Science and Engineering, Qiqihar University, Qiqihar 161006, China

<sup>e</sup> Department of Mechanical Engineering, Hong Kong Polytechnic University, Hung Hom, Kowloon,

Hong Kong

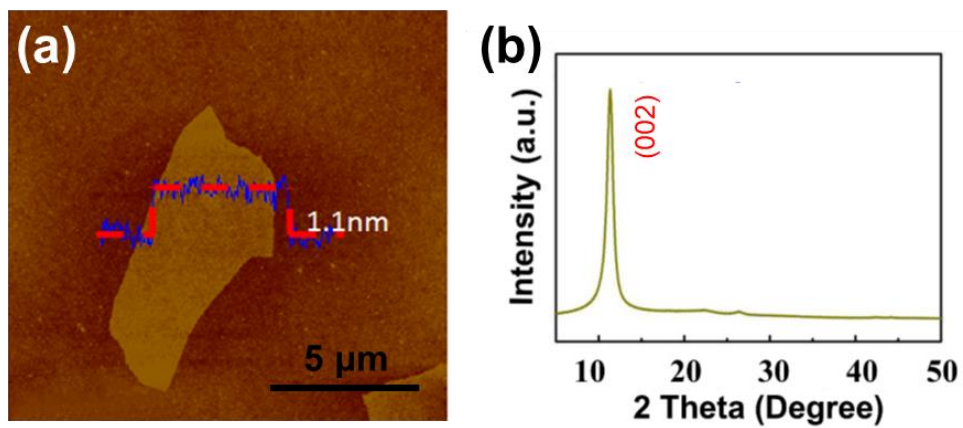


**Fig. S1** Characterization of graphene oxide (GO) sheets. **a** A tapping mode AFM image of GO sheets on a mica surface; And AFM thickness analysis on the GO membrane along the red line. **b** XRD patterns of as-prepared GO sheets.

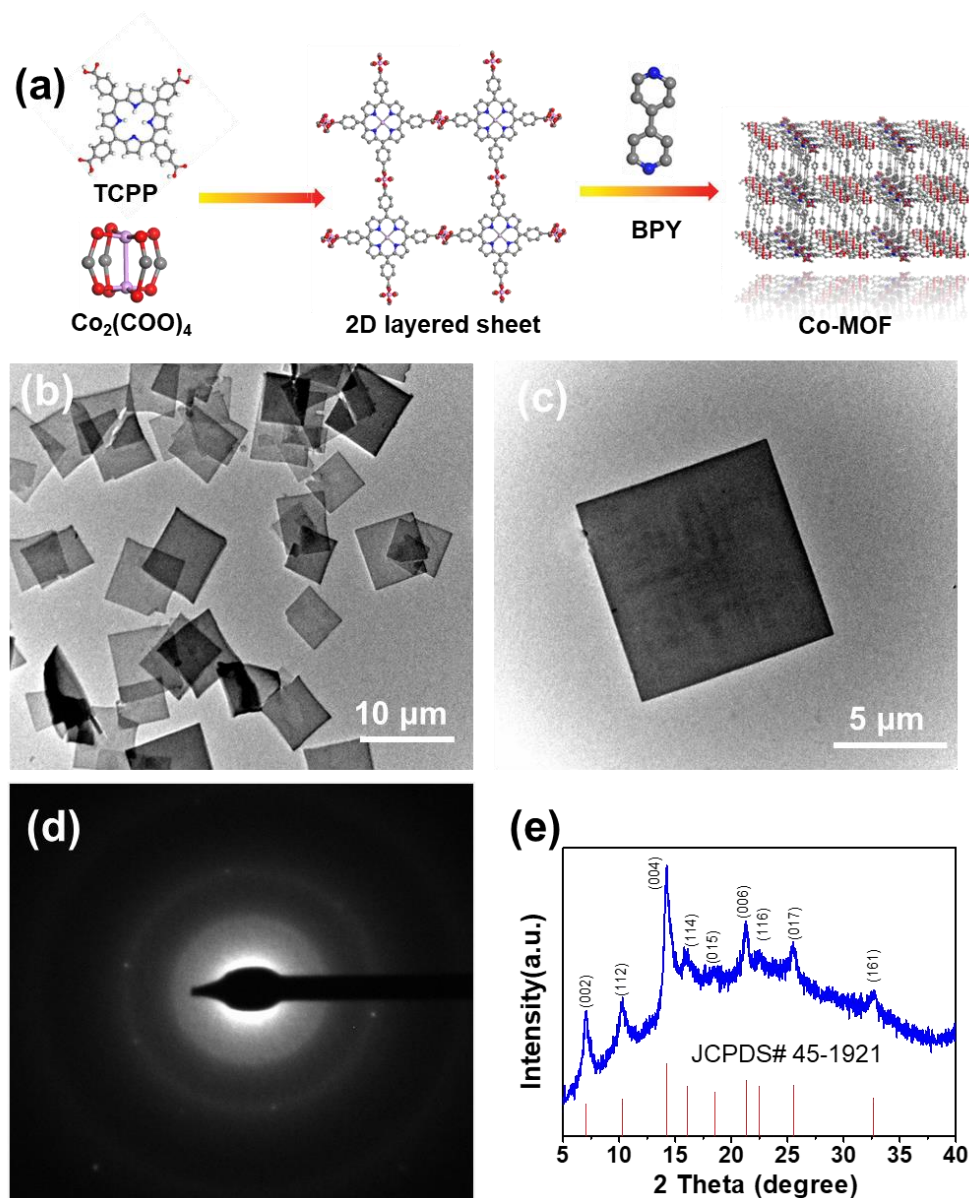


**Fig. S2** Characterization of Co-MOF nanosheets. **a** Schematic of the synthesis process of Co-MOF nanosheets. **b** TEM image of Co-MOF nanosheets. **c** TEM image of an individual Co-MOF nanosheet. **d** SAED patterns of Co-MOF nanosheets at high resolution. **e** XRD patterns of as-prepared Co-MOF nanosheets. The straight lines at the bottom of the plot are the simulated XRD patterns of the Co-MOF crystal based on the crystal structure ref. no. # 45-1921 in the JCPDS. The Co-MOF nanosheets are prepared by a bottom-up synthesis method, which is schematically shown in (a). During a typical experiment, the surfactant molecules of polyvinylpyrrolidone (PVP)

are selectively attached onto the surface of MOFs, which control the vertical growth of MOF crystals. The 5,10,15,20-tetrakis(4-carboxyl-phenyl)-porphyrin (TCPP) ligand is metalized by one cobalt ion and linked by four  $M_2(COO)_4$  ( $M = Co$ ) paddlewheel metal nodes to form a checkerboard-like layered structure, where 4,4'-bipyridine (BPY) molecules further pillar the MOF layers to form the resulting Co-MOF structure. [S1]

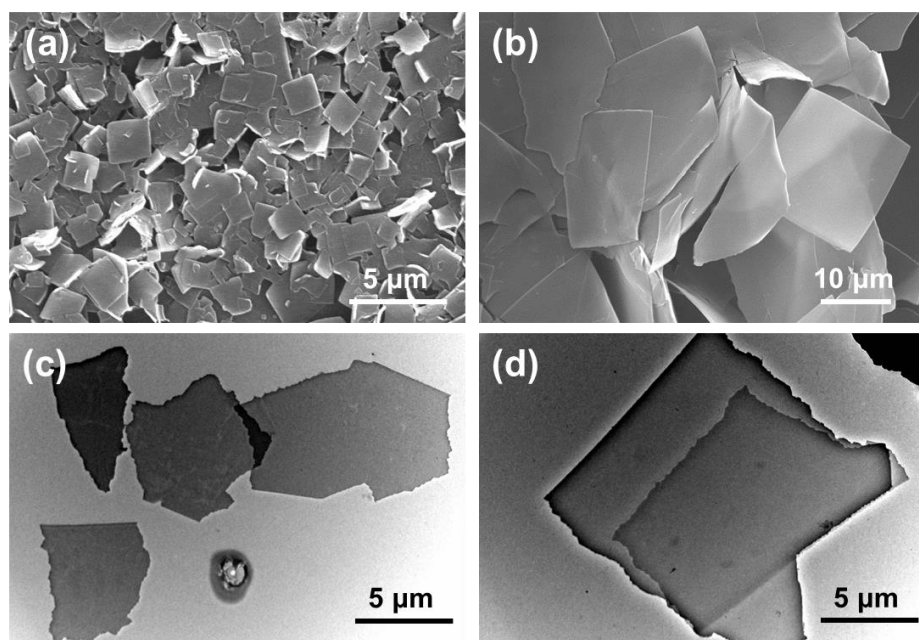


**Fig. S3** Characterization of Co-MOF nanosheets. **a** SEM image of Co-MOF nanosheets with low TCPP addition amount of 2 mg; **b** SEM image of Co-MOF nanosheets with high TCPP addition amount of 6.0 mg. **c**, **d** TEM images of Co-MOF nanosheets at low and high resolution respectively under 90 °C hydrothermal temperature conditions.

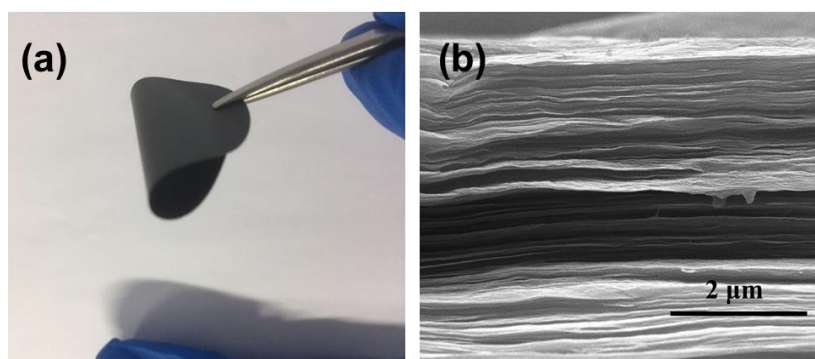


**Fig. S4** Characterization of GO membranes. **a** GO membranes obtained via a vacuum suction filter method. **b** Cross-sectional SEM image of the as-prepared GO membranes. The as-prepared freestanding GO membranes with a thickness of  $\sim 5 \mu\text{m}$  are mechanically robust and flexible, as shown in (a). The cross-sectional SEM image shows a well aligned and layered structure which is composed of numerous graphene oxide sheets densely packed with their basal planes parallel to the membrane substrates.

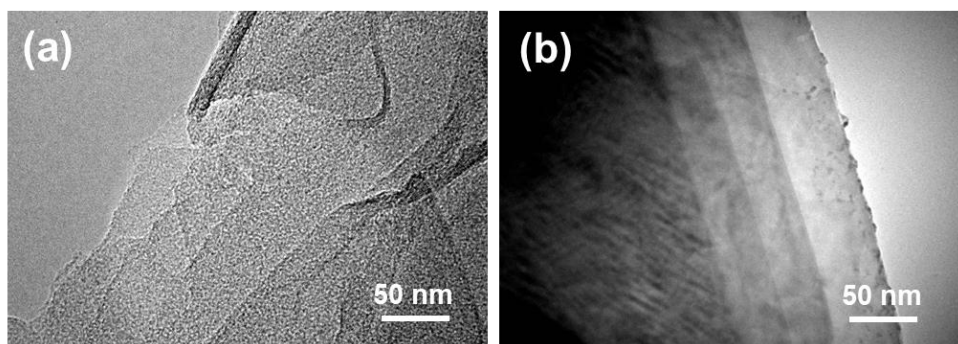


**Fig. S5** **a** Cross-sectional TEM image of the as-prepared GO membrane. **b** Cross-sectional TEM image of the as-prepared 2D Co-MOF membrane.

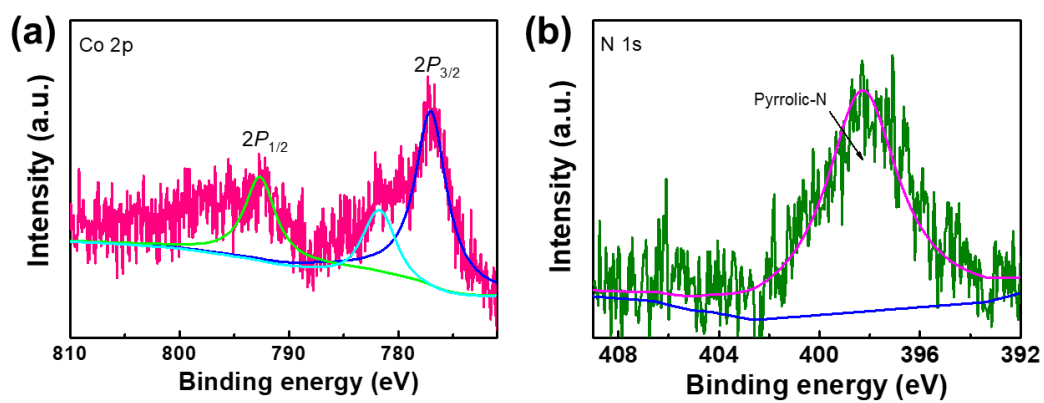


**Fig. S6** **a** Co 2p spectrum for GO/Co-MOF. **b** N 1s spectrum for GO/Co-MOF.

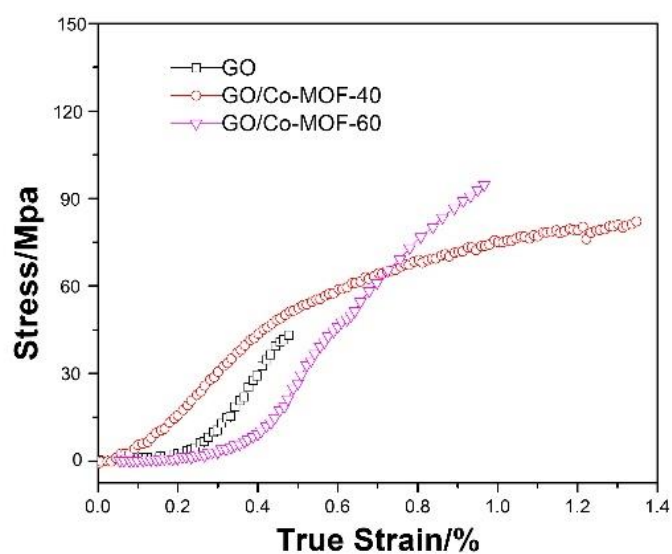
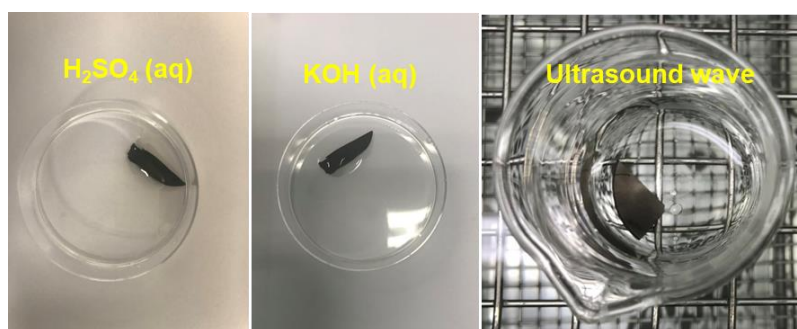


**Fig. S7** The stability of GO/2D-Co-MOF-40 membrane in 6M H<sub>2</sub>SO<sub>4</sub> solution and 6M KOH solution, and in water under agitation. For the bare GO membrane, a low tensile strength of 45.1 MPa was obtained. For the composite membranes, the mechanical strength is much higher than that of bare GO. The value is increased to 102.3 MPa for GO/Co-MOF-60, and 83.4 MPa for GO/Co-MOF-40.

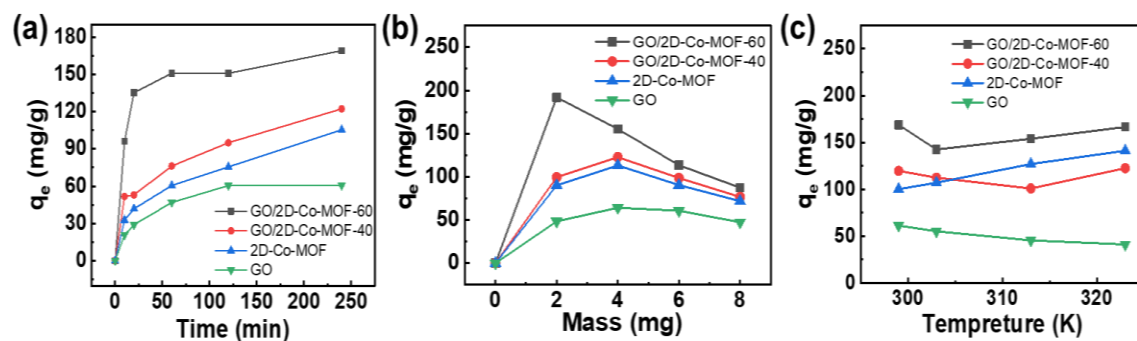


**Fig. S8** **a** Effect of contact time on the uptake quantity of  $\text{Cs}^+$  on various samples. **b** Effect of mass on the uptake quantity of  $\text{Cs}^+$  on various samples. **c** Effect of temperature on the uptake quantity of  $\text{Cs}^+$  on various samples.

**Table S1** Kinetic parameters of models for Cs<sup>+</sup> sorption on GO, Co-MOF, and GO/2D-Co-MOF-x.

R<sup>2</sup> measures the linearity of fitting in obtaining the parameters

Sample	Pseudo-first-order			Pseudo-second-order		
	k <sub>1</sub> (1/min)	q <sub>e</sub> (mg/g)	R <sup>2</sup>	K <sub>2</sub> (1/min)	q <sub>e</sub> (mg/g)	R <sup>2</sup>
GO	0.035	56.7	0.98656	0.026	58.11	0.98225
Co-MOF	0.095	67.44	0.98672	0.085	68.9	0.9921
x=40	0.67	69.4	0.93153	0.056	95.4	0.93126
x=60	0.86	96.1	0.94886	0.073	155.2	0.98764

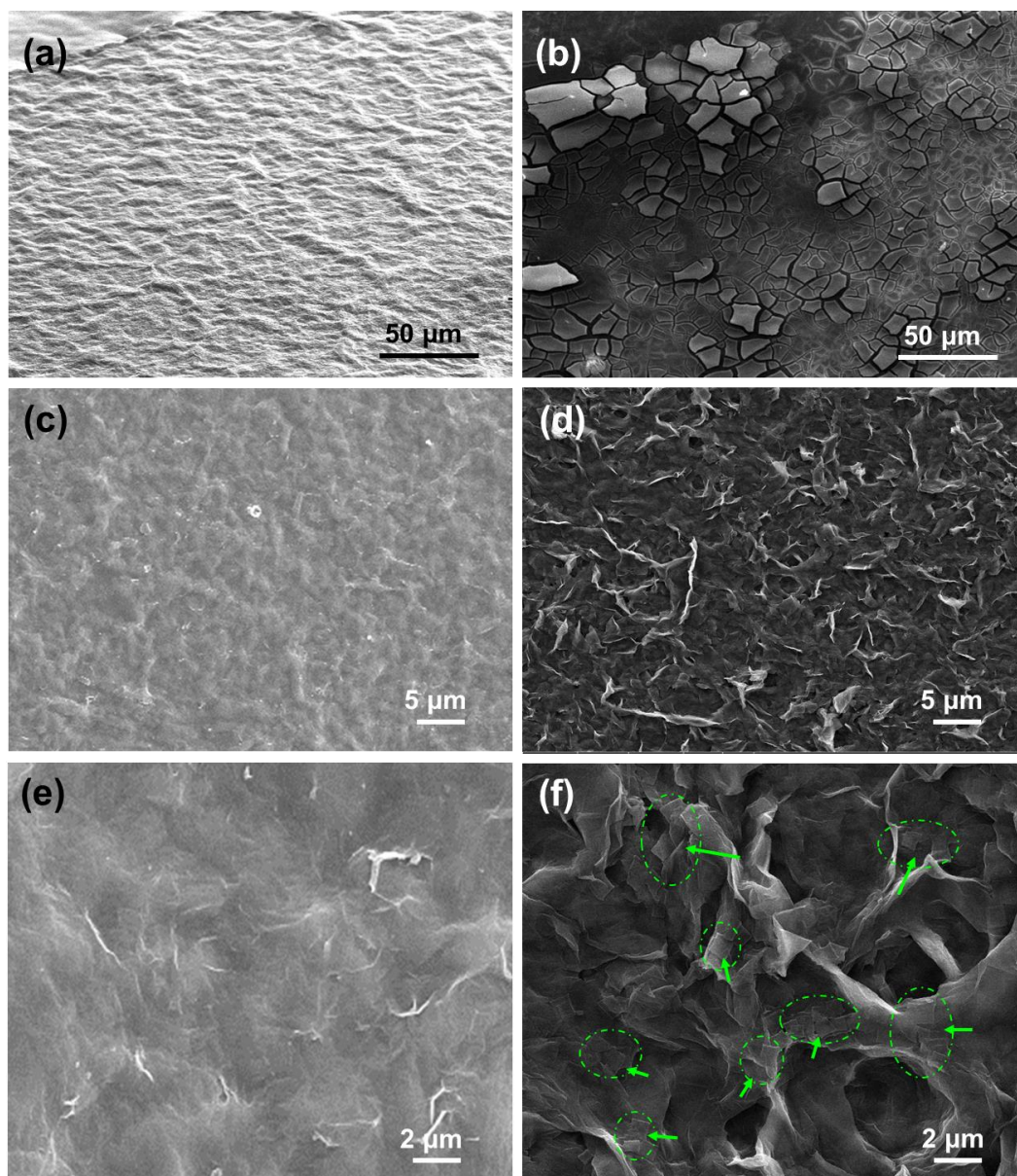


**Fig. S9** **a, c** The SEM images of GO/2D-Co-MOF-60 composite membranes before absorption of Cs<sup>+</sup>; **e** high-resolution SEM graph for GO/2D-Co-MOF-60. **b, d** The SEM images of GO/2D-Co-MOF-60 composite membranes after absorption of Cs<sup>+</sup>; **f** high-resolution SEM image for GO/2D-Co-MOF-60.

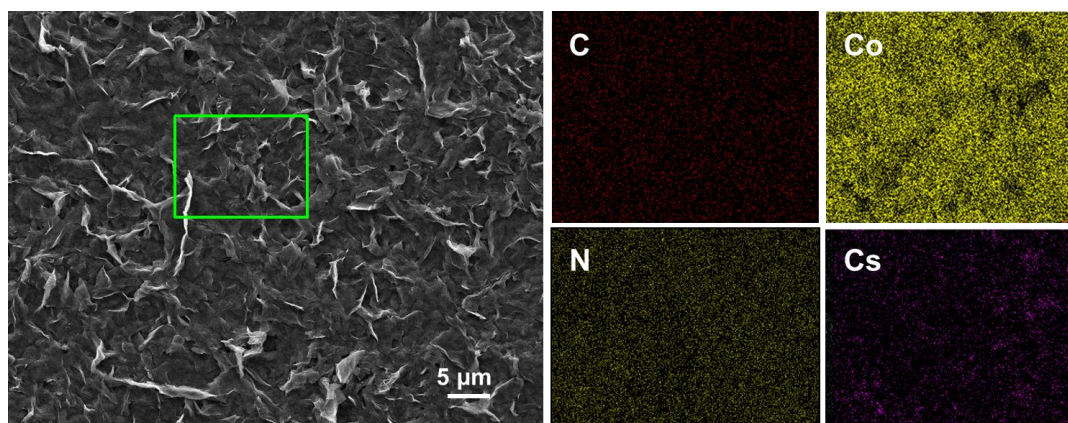


**Fig. S10** The SEM images of GO/2D-Co-MOF-60 after absorption of  $\text{Cs}^+$  and its corresponding EDS mapping patterns for C, Co, N and Cs elements.

## References

- [S1] F.F. Cao, M.T. Zhao, Y.F. Yu, B. Chen, Y. Huang, J. Yang, X.H. Cao, Q.P. Lu, X. Zhang, Z.C. Zhang, C.L. Tan, H. Zhang. Synthesis of two-dimensional  $\text{CoS}_{1.097}$ /nitrogen-doped carbon nanocomposites using metal-organic framework nanosheets as precursors for supercapacitor application. *J. Am. Chem. Soc.* **138**(22), 6924 (2016). <https://doi.org/10.1021/jacs.6b02540>
- [S2] M.A. Pimenta, G. Dresselhaus, M.S. Dresselhaus, L.G. Cancado, A. Jorio, R. Saito. Studying disorder in graphite-based systems by Raman spectroscopy. *Phys. Chem. Chem. Phys.* **9**(11), 1276 (2007). <https://doi.org/10.1039/B613962K>